Eur. Phys. J. E (2012) **35**: 50
DOI 10.1140/epje/i2012-12050-9

THE EUROPEAN PHYSICAL JOURNAL E

Regular Article

Lyotropic mixture made of potassium laurate/1-undecanol/K_2SO_4/water presenting high birefringences and large biaxial nematic phase domain: a laser conoscopy study

E. Akpinar[1], D. Reis[2], and A.M. Figueiredo Neto[2,a]

[1] Abant Izzet Baysal University, Arts and Sciences Faculty, Department of Chemistry, 14280, Bolu, Turkey
[2] Universidade de São Paulo, Instituto de Física, caixa postal 66318, 05314-970, São Paulo, SP, Brasil

Received 15 February 2012 and Received in final form 18 April 2012
Published online: 22 June 2012 –

Abstract. The lyotropic liquid crystalline quaternary mixture made of potassium laurate (KL), potassium sulphate, 1-undecanol and water was investigated by experimental optical methods (optical microscopy and laser conoscopy). In a particular temperature and relative concentrations range, the three nematic phases (two uniaxial and one biaxial) were identified. The biaxial domain in the temperature/KL concentration surface is larger when compared to other lyotropic mixtures. Moreover, this new mixture gives nematic phases with higher birefringence than similar systems. The behavior of the symmetric tensor order parameter invariants σ_3 and σ_2 calculated from the measured optical birefringences supports that the uniaxial-to-biaxial transitions are of second order, described by a mean-field theory.

1 Introduction

From the experimental point of view, the biaxial nematic phase (N_B) domain in lyotropic liquid crystals is located mainly between the two uniaxial discotic nematic (N_D) and calamitic nematic (N_C) phase domains. After the theoretical prediction [1] and experimental realization [2] of this phase in the mixture of potassium laurate (KL)/1-decanol (DeOH)/water, some research groups prepared new mixtures presenting the biaxial nematic phase. However, up to date, only eight lyotropic mixtures were experimentally found to exhibit the biaxial nematic phase [2–10].

Yu and Saupe reported the first experimental evidence of the N_B phase in 1980 [2]. They investigated the uniaxial-to-biaxial phase transitions in mixtures of KL/DeOH/water via optical conoscopy and nuclear magnetic resonance spectroscopy (NMR). Their study showed experimentally, for the first time, that the biaxial nematic is located between the domains of the two uniaxial nematic phases, as theoretically predicted by statistical models [1, 11–16]. In 1982, Bartolino *et al.* investigated the lyotropic mixture of sodium decyl sulphate (SdS)/DeOH/H_2O, which also exhibits the biaxial nematic phase [4]. Other research groups produced new lyotropic mixtures also presenting the N_B phase, namely, the mixture of rubidium laurate (RbL)/DeOH/H_2O [5], KL/decylammonium chloride (DACl)/H_2O [6], SdS/sodium sulphate (Na_2SO_4)/DeOH/H_2O [7], sodium dodecyl sulphate (SDS)/DeOH/H_2O [8], sodium lauryl sulphate (SLS)/1-hexadecanol (HDeOH)/H_2O [9] and tetradecyltrimethylammonium bromide (TTAB)/DeOH/H_2O [10]. It is interesting to point out that in all these mixtures presenting the N_B phase there are a surfactant and a co-surfactant [17]. In addition, these mixtures exhibit similar textures under polarizing light microscope and topology of phase diagrams.

From the optical point of view, an important parameter for liquid crystals is the optical birefringence [18,19]. In the case of uniaxial nematics, only one birefringence exists. The N_B phase, however, has an orthorhombic symmetry, and two birefringences have to be considered (in the following we will define more precisely these birefringences). This phase has three different indices of refraction, along the three orthogonal symmetry axes, each one of these axes of order two [20]. The nematic phases are characterized by an order parameter that is a second-rank, symmetric and traceless tensor. For practical reasons the optical dielectric tensor may be chosen as the order parameter. It can be determined by measuring the differences between the refractive indices (*i.e.*, the birefringences [21]) in the nematic phases. Moreover, the temperature dependence of the birefringences is very useful for the determination of the transition temperatures between the uniaxial and biaxial nematics to build up the phase diagram and investigate the characteristics of the phase transitions. The experimental studies on the temperature dependence of the birefringences showed that the uniaxial-to-biaxial transitions are of second order [21].

[a] e-mail: afigueiredo@if.usp.br

Although there are different techniques to establish the phase diagram topology, the most employed are the polarized optical microscopy (POM), laser conoscopy, nuclear magnetic resonance (NMR), X-ray and neutron scattering and diffraction. The phase diagrams of lyotropic mixtures published in the literature up to date, in general, were similar in terms of the temperature range of the biaxial phase and maximum value of the nematic birefringence ($\sim 2 \times 10^{-3}$) [21]. We expect that the higher the birefringence value, the more anisometric the micelles should be, and/or the different molecules that build up the micelles are more spatially segregated, and some of the biaxial features could be enhanced. The search for high birefringent biaxial samples and mixtures which present larger biaxial domains has attracted the attention of many experimentalists in the physical-chemistry of liquid crystals for several decades after Saupe's lyotropic mixture was discovered. Moreover, mixtures with those characteristics, easy to be prepared and highly reproducible are necessary to be used in complementary experiments to investigate fundamental behaviors of this remarkable nematic phase.

In this study we present a particular surface of the phase diagram of a new lyotropic mixture of potassium laurate (KL), potassium sulphate (K_2SO_4), 1-undecanol (UndeOH) and water. This mixture showed higher birefringence and larger biaxial temperature range than the mixtures exhibited in the literature. Optical microscopy and laser conoscopy experimental techniques were used to characterize the phases.

2 Experimental

Lauric acid [Merck], K_2SO_4 [Fischer], 1-undecanol (UndeOH) [Merck] were from commercial origin, used without further purification, and water-based ferrofluid [Ferrotec]. The potassium laurate (KL) was synthesized by the neutralization of lauric acid with potassium hydroxide and it was recrystallized for further purification with ethanol several times. The lyotropic nematic mixtures were prepared by weighting KL, K_2SO_4, UndeOH and water in test tubes, whose compositions are given in table 1. The mixtures were homogenized by mixing with vortex and then, from time to time, centrifuging. The tubes were put in a water bath at 40–50 °C to obtain well-homogenized mixtures. This homogenization and sample preparation was completed in 8–10 hours and then the samples were kept overnight at room temperature. Next day, a small amount of water-based ferrofluid, which was freshly prepared from the stock solution by diluting with water four times, was added to the mixture as $\sim 1\,\mu$L ferrofluid per 1 g of mixture, and the test tube was turned continuously until all ferrofluid was homogeneously dispersed in the mixture. The complete homogenization of the mixture is a key point to get reproducible results. Experimentalists must be extremely careful in the preparation of a stable lyotropic mixture. After the homogeneous mixture with ferrofluid was obtained, some amount of the sample was transferred into a 0.2 mm thick glass-flat microslide to investigate the textures under polarizing light microscope.

Table 1. Molar fractions (X) of each compound in the different lyotropic mixtures. Δn_b is defined as $\Delta n_b = \Delta n - \delta n$ in the biaxial nematic phase, at $T = 15\,^{\circ}$C.

Mixture	X_{KL}	$X_{\mathrm{K_2SO}}$	X_{UndeOH}	$X_{\mathrm{H_2O}}$	$\Delta n_b \times 10^{-3}$
1	0.0356	0.0060	0.0114	0.9470	−0.22
2	0.0365	0.0061	0.0114	0.9460	1.18
3	0.0369	0.0060	0.0114	0.9457	1.87
4	0.0383	0.0060	0.0114	0.9443	-

The laser conoscopy technique [21,22] was employed for the measurement of the optical birefringences of the nematic phases. For this purpose, the mixtures doped with ferrofluid were put in the sample cell made of two circular optical glasses, and a glass o-ring, leaving a liquid crystalline film 1.0 mm thick. Sample's birefringences were measured as a function of temperature (T). The experimental setup has a HeNe laser ($\lambda = 632.8$ nm), a Neocera LTC-21 temperature controller (which controls the temperature with an accuracy of 0.001 °C) and a Walker Sci. electromagnet that provides the static magnetic field ($|\overrightarrow{H}| = 2.04$ kG) used to orient the sample. The laboratory frame axes were defined as follows: the horizontal plane was defined by the two orthogonal axes 1 and 2; the magnetic field was aligned along the axis 1; axis 3 was vertical and parallel to the laser beam propagation direction.

Since the orientation of the nematic phases is a key point to obtain successful results in the birefringences measurements, we applied an external magnetic field in the sample. It is known that the orientation of each nematic phase with respect to the external magnetic field is different from each other. This situation was discussed, for example, by Nicoletta and co-workers [23], analyzing the typical deuterium NMR spectra of D_2O present in the mixture. In this study they investigate the three-nematic phases from a similar lyotropic mixture composed of KL/DACl/D_2O. In our case the birefringence measurements were performed starting from the N_D phase, in the presence of the magnetic field. To obtain a well-aligned N_D phase, the samples were kept at a fixed temperature for a period of time of about 30–60 min. Then, the temperature was varied step by step, depending on the proximity of the phase transition temperature: the nearer the transition temperature, the narrower the step. At each new temperature the sample was left at rest for least 10 min, in order to achieve the thermal equilibrium. From time to time, in the N_D (N_B) phase, the sample was turned by an angle of about $\pm\pi/2$ ($\pm\pi/6$) around axis 3 to improve the sample orientation. Let us discuss this procedure in more details. As the anisotropy of diamagnetic susceptibility of our N_D phase is negative, the director $\overrightarrow{n}$ orients perpendicularly to $\overrightarrow{H}$. However, there is a degeneracy in the orientation of the director, because $\overrightarrow{n}$ can be in any direction in the plane perpendicular to $\overrightarrow{H}$. To break this degeneracy we spin the sample around the axis 3 by $\alpha = \pm\pi/2$ in the presence of the field, staying at each orientational configuration for about one minute. With this

procedure, after some spins, the degeneracy is broken and $\overrightarrow{n}$ orients parallel to the spinning axis. Before any measurement of the birefringences (at $\alpha = 0$) we check the quality of the interference fringes that, in this nematic phase, are composed of circular rings centered in the axis 3, and two straight lines perpendicularly oriented. We observed that the sample keeps its orientation for minutes, a sufficient time to perform the measurement. This procedure is repeated at each temperature. In the case of the N_B phase the magnetic field orients one of its symmetry axis parallel to the field, however, the other symmetry axes, perpendicular to this one, remain in the plane perpendicular to the field, without a preferred orientation direction. We observed that the N_B phase encapsulated in flat glass microslides in the presence of an external magnetic field applied in the largest surface of the microslide, presents under crossed polarizers, a planar-like texture. This result indicates that one of the symmetry axis of the N_B phase orients perpendicular to the glass flat surface, and the other symmetry axis orients parallel to the field. In the case of our sample-holder cell, to break the initial orientational degeneracy, improve the orientation of the phase axis perpendicular to the flat glass surface, and obtain a sample oriented with the three orthogonal symmetry axes parallel to the laboratory frame axes, we spin the sample around axis 3 by an angle of about $\alpha = \pm\pi/6$, in the presence of the field. This procedure defines a new direction, perpendicular to the magnetic field, along which another of the phase's symmetry axis will orient. Not to lose the orientation of the axis parallel to the field, the spinning is done as follows: 60 seconds at $\alpha = 0$, 30 seconds at $\alpha = \pi/6$, 30 seconds at $\alpha = -\pi/6$ and 60 seconds at $\alpha = 0$. The procedure is repeated until the conoscopic pattern reaches a stationary state at $\alpha = 0$, with the fringes symmetric and well contrasted. This empirical procedure, which combines the magnetic field and a spinning axis perpendicular to it, was shown to orient the N_B phase [22].

The laser conoscopy furnishes the two main optical birefringences, $\Delta n = n_2 - n_1$ and $\delta n = n_3 - n_2$, which were measured as a function of temperature. The birefringences were obtained by measuring the refraction angles of the interference figures (isogyres or isochromates) in the plane perpendicular to the laser propagation direction [24].

3 Results and discussion

3.1 Polarizing light microscopy

The typical textures observed (from mixture 4) between crossed polarizers in the phases N_D, N_B and N_C are shown in fig. 1a, b, c, respectively. The schlieren textures clearly identify the nematic topology, however, only from these textures it is very difficult to identify undoubtedly the particular nematic phase. This is particularly true in the case of the textures from the N_B and N_C phases. At lower (higher) temperatures we observed that the N_B (N_D) phase transit to a two-phase (multi-phase) region, which is not the main interest of the present study. The texture of the two-phase region can be seen in fig. 1d, where isotropic black droplets start to appear, besides birefringent colored regions with sharp edges. These birefringent domains may correspond to crystalline phases, but the texture alone is not enough to characterize it. The texture of the multiphase region is shown in fig. 1e. N_D, isotropic and high birefringent domains (probably a lamellar phase) are visible. The typical textures of the N_B and N_D phases, and the two-phase region shown in fig. 1 were also observed in mixtures 1, 2 and 3 from table 1. To establish the phase diagram of our mixture, as a function of the temperature, it is necessary to use additional experimental techniques. The laser conoscopy will be discussed in the following.

3.2 Laser conoscopy

As pointed out before, laser conoscopy is a very powerful technique to determine the optical birefringences of all nematic phases [21,22], but the sample orientation is a key point to perform a precise measurement. For this purpose and to improve the effect of the magnetic field on the different samples, a small amount of water-based ferrofluid was added to the mixtures. We verified that the transition temperatures did not change (within our accuracy) as a consequence of this ferrofluid doping. This result is already known from the literature for other lyotropic mixtures [17]. To be sure that the values of the birefringences measured in the ferrofluid-doped mixtures are the same as the undoped mixtures, we performed control experiments. The first one was to prepare a sample that presents an isotropic phase, dope it with the same amount of ferrofluid, and measure the birefringences. We verified that within the experimental errors (see the error bars in fig. 2) the birefringences are zero. This indicates that there is no residual birefringence due to the magnetic particles present in the sample. Another experiment consisted in measuring the sample birefringences in the N_C phase without the ferrofluid, oriented by a strong magnetic field (of the order of 10 kG), and compare them with those measured at 2.04 kG with the ferrofluid-doped sample. Again, the values of the birefringences measured were the same, taking into account the experimental errors. As the attainment of well-oriented samples to measure the birefringences is a key point in this work, let us give more details about it. It is known that micelles composed of soaps with hydrocarbon chains tend to orient these chains perpendicular to the magnetic field [25]. Using a combination of different elements (magnetic field with the ferrofluid doping and surface effect) and procedures (periodic rotations along the z-axis) the good orientation of the different nematic phases is achieved. In the particular case of the N_B and N_D phases, the surface effect helps to orient the entire sample, since the micellar symmetry axis perpendicular to the largest surface of the micelles tends to orient perpendicular to the glass surfaces. In the N_B phase, besides the effect described above, the magnetic field orients a second micellar symmetry axis parallel to it. To check if the laser beam is reaching a well-oriented monodomain in the laser conoscopy experiment, we have just to inspect the shape of the interference pattern: well-oriented samples

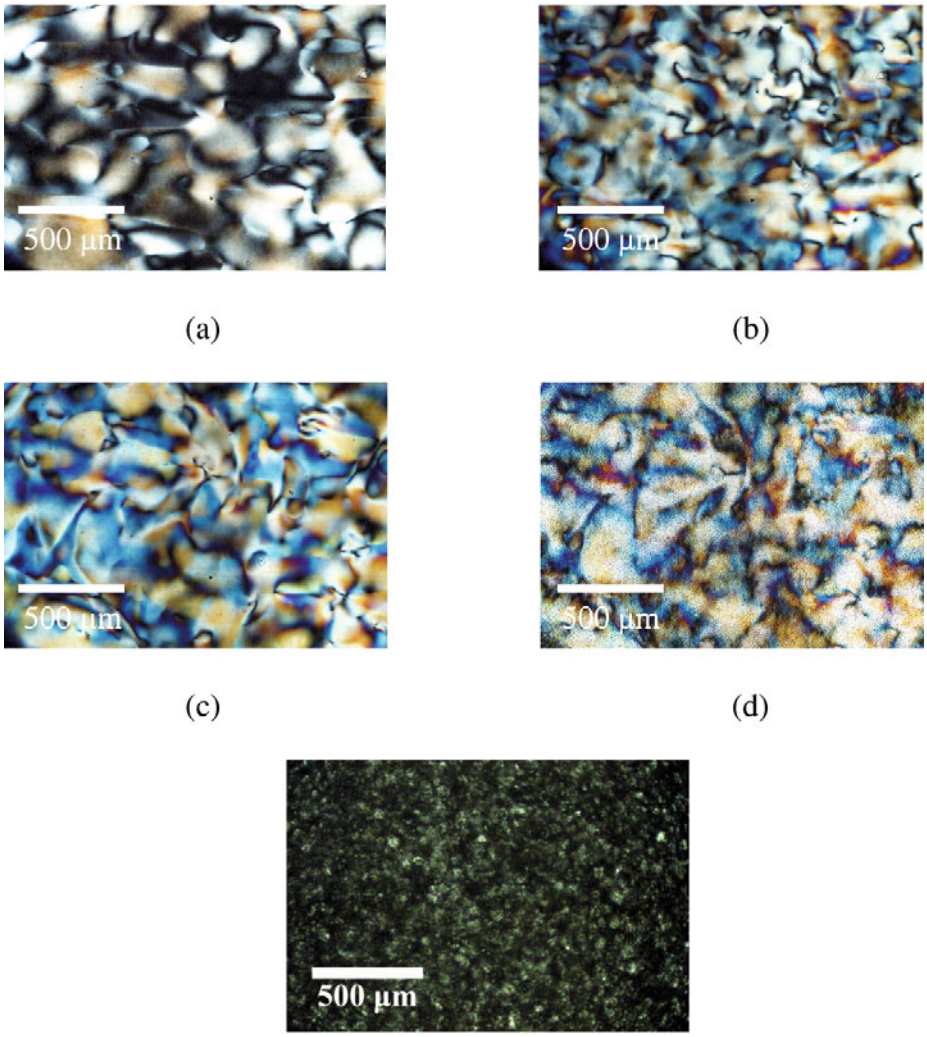

Fig. 1. Typical optical microscopy textures, under crossed polarizers, of mixture 4: a) N_D phase, $T = 45\,^{\circ}C$; b) N_B phase, $T = 27.5\,^{\circ}C$; c) N_C phase, $T = 15\,^{\circ}C$; d) two-phase region, $T = 10.2\,^{\circ}C$, e) multi-phase region, $T = 60\,^{\circ}C$.

give symmetric and highly contrasted light and dark regions (isogyres or isochromates). The measurements were performed only when these conditions were verified.

Since the mixtures of KL/K_2SO_4/UndeOH/H_2O show the N_D phase at higher temperatures, the optical birefringences of each nematic phase as a function of temperature were measured starting from the N_D phase, upon cooling. The experimental results of Δn and δn as a function of T, from the mixtures 1-4 (see table 1), are shown in fig. 2. The plot of the birefringences clearly identifies the different uniaxial (when one of the birefringences is zero) and the biaxial (when both birefringences are different from zero) phases. In fig. 3 we sketched the particular surface of the phase diagram of the mixture KL /K_2SO_4/UndeOH/ water, keeping the molar fractions of UndeOH and K_2SO_4 constant. Increasing the molar fraction of KL we observe a decrease of the N_B domain and the appearance of the N_C phase domain. Surprisingly, the N_D phase domain is located at higher temperatures, differently from the usual KL/DeOH/water mixture. In parallel we verified that the ternary system KL/UndeOH/water shows a very similar phase diagram to the usual KL/DeOH/water system (these new samples were prepared with about the same molar fraction as UndeOH with respect to that of the DeOH). The nematic-to-nematic transition temperatures in the ternary system with UndeOH shifted to higher temperatures when compared to those with DeOH. This situation may be related to the different location of the polar head, -OH, of both alcohols near the head group of the KL on the micelle surface, but it has to be investigated in more details with complementary techniques. In both systems (with UndeOH or DeOH) we verified that the addition of salt favors the stabilization of the N_D phase at higher temperatures, *i.e.*, the phase sequence as a function of temperature inverts. In particular, the quaternary system with UndeOH gave smaller N_B phase domain when compared with the quaternary mixture with DeOH.

A particular surface X_{KL} *versus* T (at $X_{K_2SO_4} = 0.0060$ and $X_{UndeOH} = 0.0114$) of the phase diagram of our new mixture is sketched in fig. 3. While the mixtures 1, 2 and 3 gave the nematic N_D and N_B phase, mixture 4 presented N_C phase domain in addition to the those

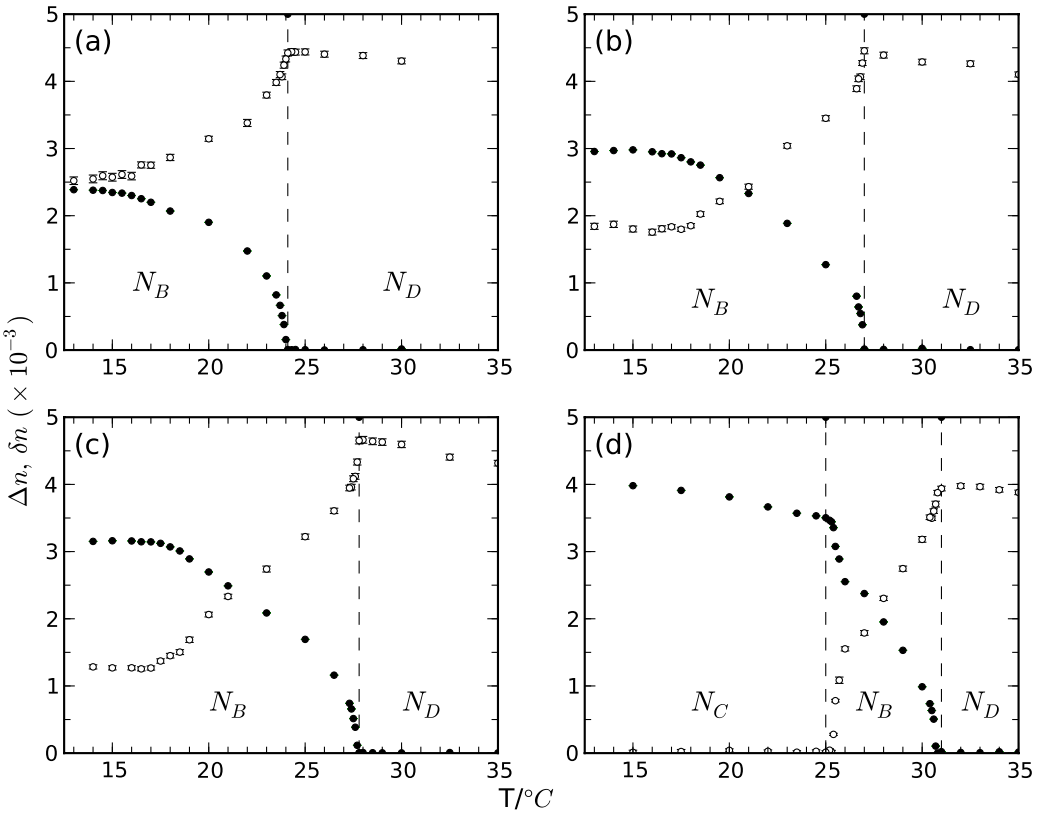

Fig. 2. Birefringences of the different mixtures of KL/K_2SO_4/UndeOH/H_2O as a function of the temperature. $\Delta n = n_2 - n_1$ (•) and $\delta n = n_3 - n_2$ (○). a) Mixture 1; b) mixture 2; c) mixture 3; d) mixture 4.

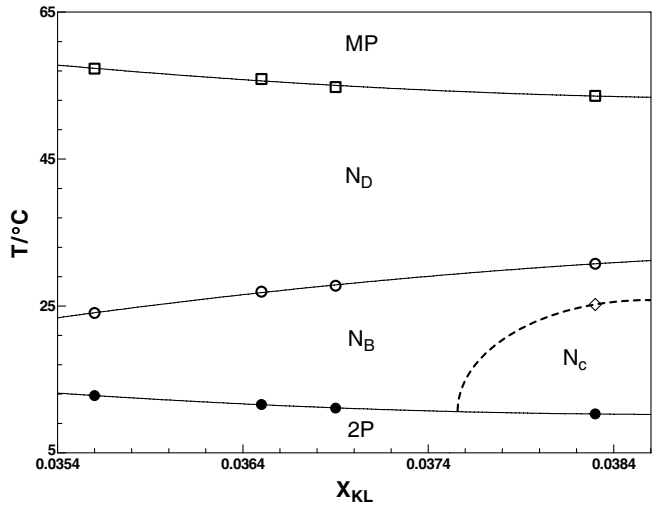

Fig. 3. Surface X_{KL} *versus* T (at $X_{\mathrm{K_2SO_4}} = 0.0060$ and $X_{\mathrm{UndeOH}} = 0.0114$) of the phase diagram of the mixture KL/K_2SO_4/UndeOH/H_2O. Solid lines are guide for the eyes, and the dashed line represents qualitatively the beginning of the N_C domain at higher molar fractions of KL. The label 2P and MP represent a two-phase and a multi-phase regions, respectively.

domains. In the case of higher temperatures, above the N_D, for all mixtures, a multi-phase, MP, domain was observed.

At this point, before discussing the experimental results in more details, we will briefly review some phenomenological models concerning the biaxial nematic phase. By this way we may discuss qualitatively some microscopic aspects of the micelle in our new lyotropic mixture with respect to other known mixtures. After Yu and Saupe reported the first biaxial nematic phase a question arises: is there a mixture of disk-like and cylindrical-like micelles in the N_B? In 1984, Stroobants and Lekkerkerker proposed a model where cylindrical and discotic objects coexist, giving rise to the biaxial nematic phase [26]. This type of model, however, had many problems. From the theoretical point of view it has been shown that such a mixture of cylindrical and discotic objects was indeed unstable and should necessarily demix [27,28]. Kooij and coworkers experimentally showed that systems composed of a mixture of disk-like and cylindrical-like objects demix, without giving rise to a N_B phase [29]. These papers quoted before [26–29] deal with rigid objects, and should be more appropriate to support the fact that, up to date, there is not in the literature an example of mixtures of disk-like and cylindrical nano-objects, or even molecules, giving rise to the N_B phase. The case of lyotropics is more complicated because micelles are not rigid objects. Amphiphilic molecules exchange between micelles and even between them and the bulk. The lifetime of an amphiphilic molecule in a micelle is of the order of 10^{-5}–10^{-3} s [30]. At the time scale of the optical or X-ray diffraction ex-

periments (at least, minutes) we expect that the micelles present a fixed shape. Recently a theoretical attempt to stabilize a N_B phase with a mixture of disks and cylinders was done [31]. To prevent the occurrence of demixing, it was suggested that, if such a mixture is cooled down at a lower temperature than the orientational degrees of freedom, some translational ones freeze by about 30 K. Such hypothesis with two different temperatures in the same system is purely theoretical, and cannot be realized experimentally. Consequently, the existence of mixtures of disk-like and cylindrical-like micelles in the biaxial nematic phase has no theoretical or experimental support, and we will disfavor this approach. A different approach was proposed by Neto *et al.* [32] and Galerne *et al.* [33]. They proposed the intrinsically biaxial micelles (IBM) model, which is based on the different orientational fluctuations of the same type of micelles in the three nematic phases. In the IBM model, the micelles have an orthorhombic symmetry in the three-nematic phases, and the two uniaxial and biaxial phases arise from orientational fluctuations of the intrinsic locally biaxial micelles. Orientational fluctuations that are full rotations around the long micellar axis or along the axis perpendicular to the largest surface of the micelle give rise to the N_C and N_D phases, respectively. Small amplitude orientational fluctuations around the three-micellar axes give rise to the N_B phase. The discussion made hereafter will be based on the IBM model.

Let us come back to the phase diagram of fig. 3. The system KL/K_2SO_4/UndeOH/water shows a N_D phase domain at higher temperature and, on cooling, we observed a transition to the N_B phase. At lower concentrations of KL (mixtures 1-3) the N_B phase remains at lower temperatures, without transiting to the N_C phase, fig. 2a-c. In the framework of the IBM model, continuous modifications in the shape anisotropy of the micelles as a function of the temperature trigger the different orientational fluctuations that give rise to the nematic phases and phase transitions. The inexistence of a transition to the N_C phase on cooling, at lower KL mole fractions, indicates that locally the micelles did not reach the characteristic shape anisotropy which favors the orientational fluctuation which degenerates the axis parallel to the biggest micellar dimension. In other words, the shape anisotropy is "frozen" in the biaxial domain. On the other hand, increasing the KL mole fraction, the micellar shape anisotropy reaches the value necessary to form the N_C phase. This result is consistent to the picture that increasing the KL concentration increases the largest micellar dimension, *i.e.*, the micelle became more elongated. This assumption is consistent with the X-ray diffraction results obtained in the KL/DeOH/water mixture [33]. This more anisometric micelle in the plane of the biggest micellar surface favors the orientational fluctuation that originates the N_C phase. As shown by neutron scattering experiments [34], the KL molecules accumulate mainly on the most curved parts of the micelles, leading to an increase of the largest size of the micelle. To go further on this microscopic analysis, X-ray diffraction experiments must be performed, however, the analysis of the birefringence values can give us some hints about it.

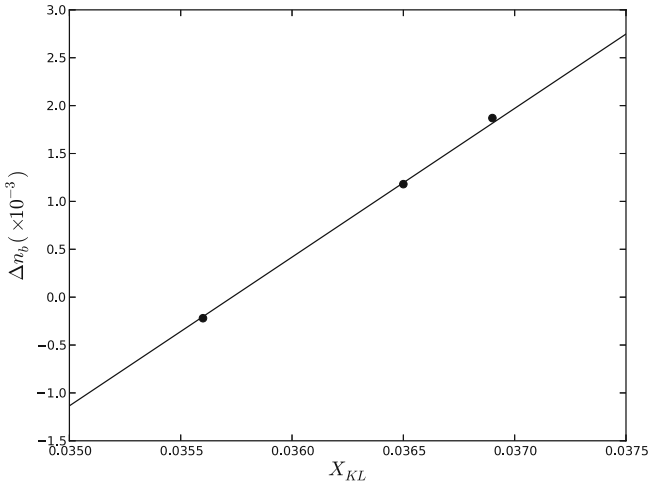

Fig. 4. Difference between two optical birefringence values $\Delta n_b = \Delta n - \delta n$, at $T = 15\,^{\circ}\mathrm{C}$ as a function of the KL mole fraction X_{KL}.

The birefringence observed in lyotropic nematics comes from different origins. The main sources of it are the anisotropic distribution of the different molecules in the micelle, the shape anisotropy of the micelles and the micellar spatial organization. It is interesting to compare the absolute value of the optical birefringences achieved in this new lyotropic mixture with those from other mixtures. In particular, in the N_D phase our quaternary mixture reaches birefringence values of about 5×10^{-3}, almost two times the maximum value encountered in the KL/DeOH/water system. In the framework of the IBM model, this result should indicate that the shape anisotropy of the micelles in our new system may be larger than that found in the usual KL/DeOH/water system. However, we cannot discard the possibility that the micelles maintain approximately the same shape anisotropy as those encountered in the KL ternary mixture, but present a steeper segregation of identical molecules in the micelle. This aspect needs further experiments of X-ray diffraction and even contrast neutron investigations, which are beyond the subject of the present work.

It can be seen from fig. 2a-c that, as the KL concentration increases, the difference between two optical birefringence values in the limit of low temperatures, $\Delta n_b = \Delta n - \delta n$, get bigger. Since the biaxial phase remained until $\sim 13.0\,^{\circ}\mathrm{C}$, the Δn_b values at the temperature of $15.0\,^{\circ}\mathrm{C}$ were plotted *versus* the mole fraction, X_{KL}, of KL in fig. 4. We observed a linear dependence of Δn_b on X_{KL}. Increasing X_{KL} the birefringence $\delta n \to 0$, and there is a tendency of the system to stabilize the N_C phase.

As pointed out before, the nematic phases of the lyotropic liquid crystals are characterized by a second-rank, traceless, symmetric tensor order parameter [1,11]. The optical dielectric tensor $\overleftrightarrow{\varepsilon}$, which has the same symmetry as the phases, can be chosen as the order parameter [18]. The diagonal elements of the anisotropic part of the dielectric tensor may be written as functions of the optical

birefringences [21,22],

$$\varepsilon_{a1} = -\frac{4\langle n\rangle}{3}\left(\Delta n + \frac{\delta n}{2}\right),$$
$$\varepsilon_{a2} = \frac{2\langle n\rangle}{3}(\Delta n - \delta n),$$
$$\varepsilon_{a3} = \frac{4\langle n\rangle}{3}\left(\frac{\Delta n}{2} + \delta n\right), \quad (1)$$

where $\langle n\rangle$ is the average index of refraction of the nematic phase and it can be determined from Abbe's refractometer. The symmetric invariants of the tensor order parameter, σ_1, σ_2 and σ_3 [1] are

$$\sigma_1 = \varepsilon_{a1} + \varepsilon_{a2} + \varepsilon_{a3},$$
$$\sigma_2 = \frac{2}{3}\left(\varepsilon_{a1}^2 + \varepsilon_{a2}^2 + \varepsilon_{a3}^2\right),$$
$$\sigma_3 = 4\varepsilon_{a1}\varepsilon_{a2}\varepsilon_{a3}, \quad (2)$$

where the first invariant σ_1 is zero. In the uniaxial phases the invariant σ_3 is related to σ_2 by $\sigma_3 = \pm\sigma_2^{3/2}$ [21]. The signs + (−) refer to the N_D (N_C) phase. In the biaxial phase, σ_3 takes values between $-\sigma_2^{3/2}$ and $\sigma_2^{3/2}$, $-\sigma_2^{3/2} < \sigma_3 < \sigma_2^{3/2}$, and this is evidence of the location of the N_B phase between the two uniaxial nematic phases.

Figure 5 shows the dependences of σ_2 and σ_3 on temperature of mixture 4 (other mixtures exhibited similar temperature dependence of the invariants). From the mean-field theory, we expect that, near the phase transitions (uniaxial-to-biaxial), σ_2 and σ_3 depend linearly on T. The Landau-de Gennes expansion of the free energy may be written as a function of these invariants, with the coefficients being functions of temperature (and concentrations) [22]. σ_2 and σ_3 are linear functions of the Landau coefficients, and therefore, of temperature. This behavior is observed in fig. 5. The mean-field characteristic of the uniaxial-to-biaxial transitions may also be seen from the behavior of the birefrigences as a function of the temperature in the vicinity of the transition temperatures (fig. 2). In fig. 6, the σ_3 values of the all mixtures were plotted against σ_2. In fig. 6, solid lines represent the σ_3 *versus* σ_2 loci of the uniaxial nematic phases: $\sigma_3 = \pm\sigma_2^{3/2}$, the signs + (−) refer to the N_D (N_C) phase. The experimental points plotted in fig. 6 were calculated from the measured Δn and δn. As a consequence of the high birefringences values our quaternary mixture achieves, the invariants of the order parameter also reach high values. In the case of the KL/DeOH/water system, $\sigma_2 \leq 2\times10^{-5}$ and $|\sigma_3| \leq 10^{-7}$. In our case the maximum values of these invariants are $\sigma_2 \sim 6\times10^{-5}$ and $|\sigma_3| \sim 4\times10^{-7}$.

Another way to show the uniaxial and biaxial characteristics of the lyotropic phases is to make suitable matches between the symmetry axis of the phases (X, Y, Z) and the principal axes of the laboratory reference frame, through the principal components of the $\overleftrightarrow{\varepsilon}$ tensor $(\varepsilon_{XX}, \varepsilon_{YY}, \varepsilon_{ZZ})$, such that the relative phase biaxiality $(\varepsilon_{XX} - \varepsilon_{YY})/\varepsilon_{ZZ}$ ranges in the interval −1 to 0 [23]. In the uniaxial phases the relative phase biaxiality is zero,

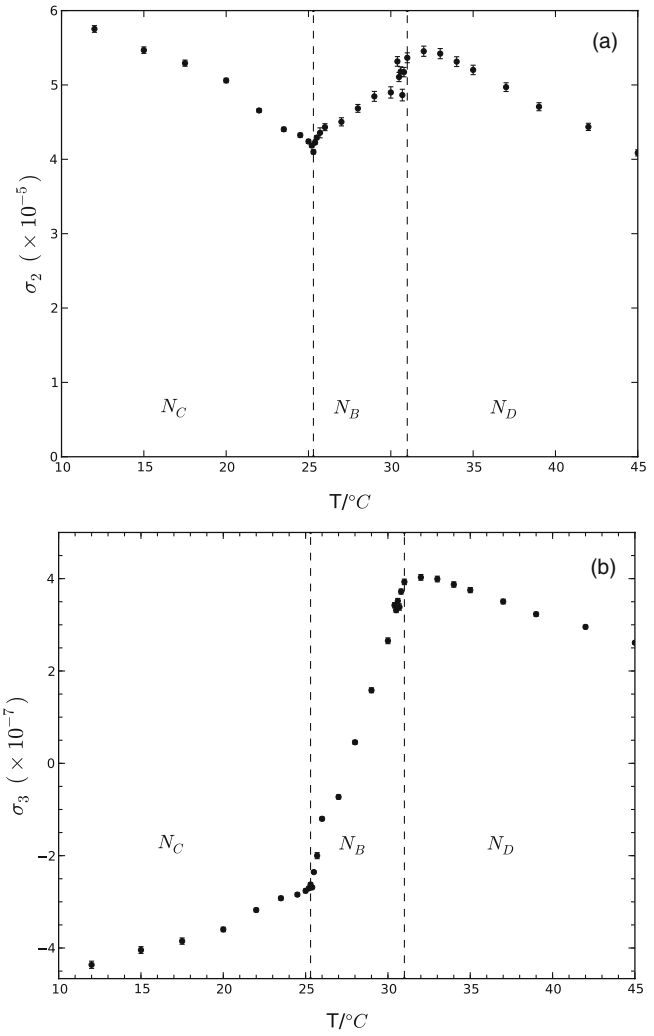

Fig. 5. Temperature dependence of the invariants of the order parameter: (a) σ_2 and (b) σ_3. Dashed lines mark the uniaxial-to-biaxial transition temperatures. Values from mixture 4.

since $\varepsilon_{XX} = \varepsilon_{YY}$ and, in the biaxial phase, it is different from zero. Its relative value gives a measure of the biaxiality. Following this definition, in the N_D phase we chose $\varepsilon_{XX} = \varepsilon_{a1}$, $\varepsilon_{YY} = \varepsilon_{a2}$ and $\varepsilon_{ZZ} = \varepsilon_{a3}$, and in the N_C phase $\varepsilon_{XX} = \varepsilon_{a3}$, $\varepsilon_{YY} = \varepsilon_{a2}$ and $\varepsilon_{ZZ} = \varepsilon_{a1}$. In the biaxial phase the axes are labeled such that, when $\delta n \geq \Delta n$ the definitions are the same as the N_D phase, and when $\delta n \leq \Delta n$ the definitions are the same as the N_C phase. The results for the relative phase biaxiality for each one of the mixtures are in fig. 7. From the plot the uniaxial and biaxial phases are immediately identified. Figure 7d, where the three-nematic phases are present, shows a similar plot as that observed in the KL/DACl/D_2O mixture [23]. However, the behavior of the relative phase biaxiality in mixtures 1, 2 and 3 is remarkable. As discussed before, these results seem to indicate a "freeze" of the micellar shape anisotropy (or even in the local molecular nanosegregation) as the temperature decreases. In the case of mixture 1 δn is greater than Δn throughout the whole N_B domain, while in mixtures 2 and 3 there are temperature

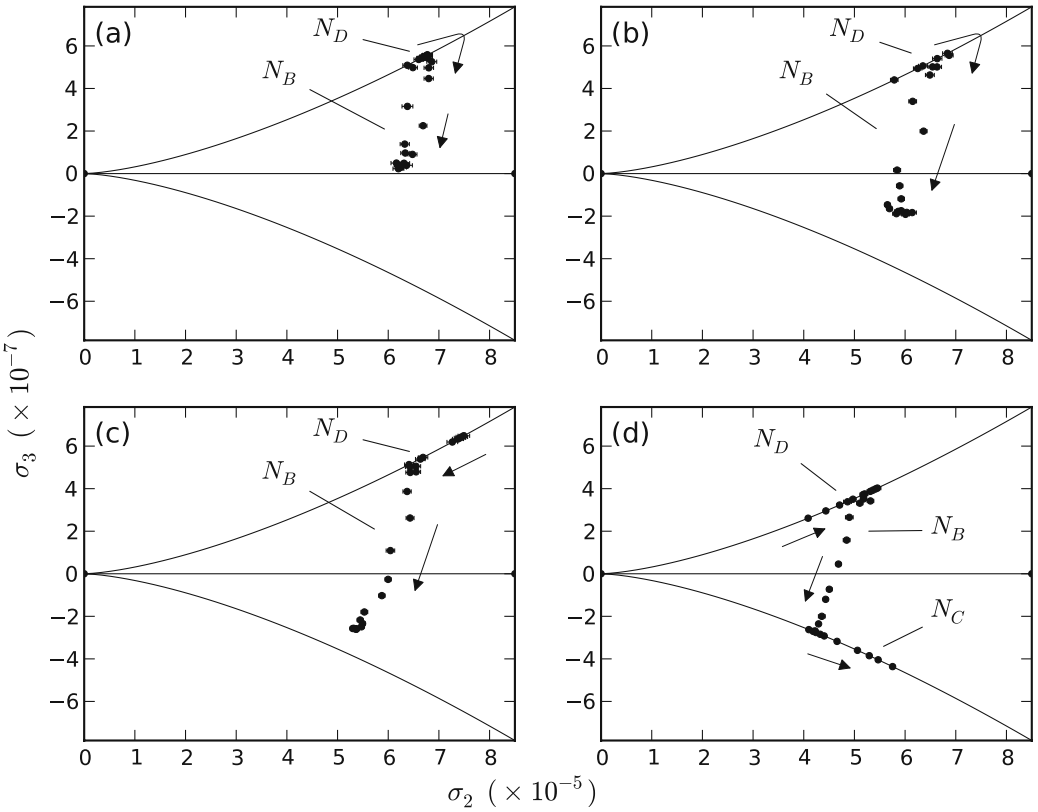

Fig. 6. The dependence of σ_3 on σ_2 for the mixtures (a) 1, (b) 2, (c) 3 and (d) 4, at the working temperature range. Solid lines represent the σ_3 *versus* σ_2 loci of the uniaxial nematic phases: $\sigma_3 = \pm\sigma_2^{3/2}$, the signs + (−) refer to the N_D (N_C) phase. The arrows indicate the cooling process employed to measure the birefringences, starting from the N_D phase.

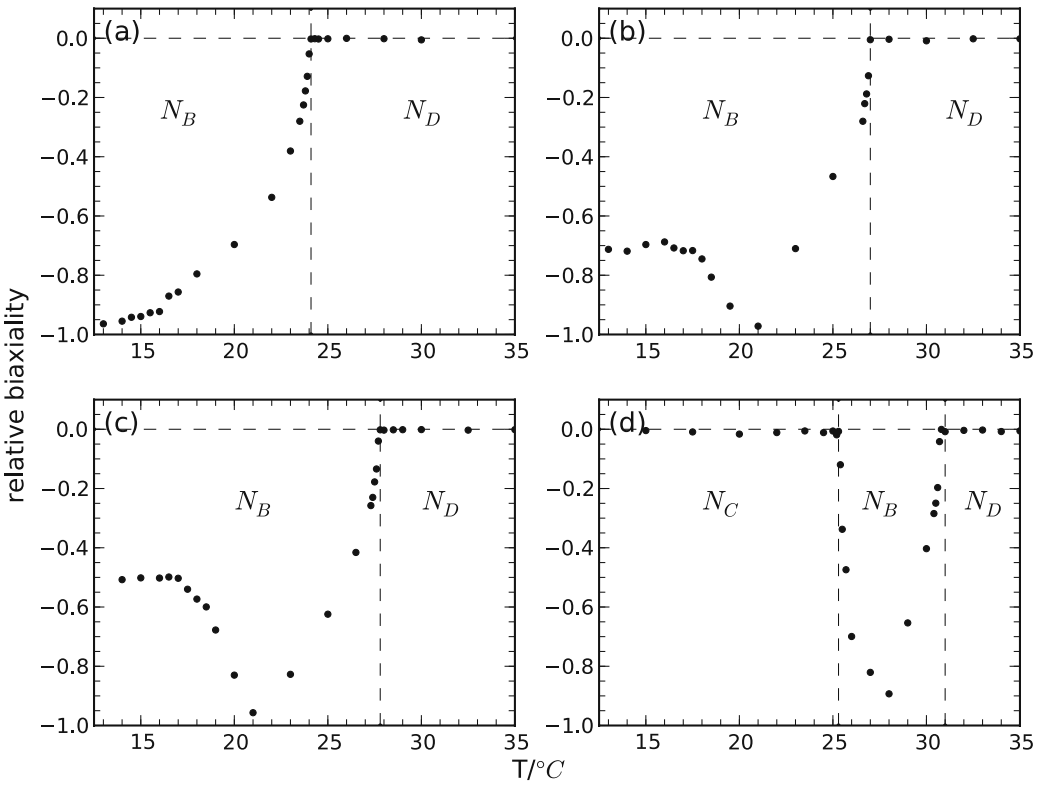

Fig. 7. Relative phase biaxiality as a function of temperature for the mixtures (a) 1, (b) 2, (c) 3 and (d) 4.

ranges where one is greater or smaller with respect to the other. In the framework of the IBM model, decreasing the temperature in the N_B phase domain, the micelles do not reach the shape anisotropy that favors the orientational fluctuation typical of the N_C phase.

4 Conclusions

A new lyotropic mixture of KL/K_2SO_4/UndeOH/H_2O showing the three nematic phases was prepared. At lower KL concentrations this mixture gives only the uniaxial discotic and biaxial nematic phases, whereas, at higher KL concentrations, it exhibits two uniaxial discotic and calamitic nematic phases and a biaxial nematic phase domain located between them. The biaxial region is stable in a larger temperature *versus* amphiphile concentration range when compared to other mixtures reported in the literature. Moreover, this new mixture gives nematic phases with high values of the birefringences comparing to other systems. This result is expected to be related to the micellar shape anisotropy and/or to a higher nano-segregation of the different molecules in the micelles. In addition, the behavior of the symmetric tensor order-parameter invariants σ_3 and σ_2 calculated from the measured optical birefringences supports that the uniaxial-to-biaxial transitions are of second-order, described by a mean-field theory.

We thank The Scientific and Technological Research Council of Turkey (TÜBİTAK) for supporting this present study. INCT and NAP on Complex Fluids, FAPESP and CNPq financial support.

References

1. M.J. Freiser, Phys. Rev. Lett. **24**, 1041 (1970).
2. L.J. Yu, A. Saupe, Phys. Rev. Lett. **45**, 1000 (1980).
3. A.M. Figueiredo Neto, L. Liebert, Y. Galerne, J. Phys. Chem. **89**, 3737 (1985).
4. R. Bartolino, T. Chiaranza, M. Meuti, R. Compagnoni, Phys. Rev. A **26**, 1116 (1982).
5. Y. Galerne, L. Liebert, Phys. Rev. Lett. **55**, 2449 (1985).
6. E.A. Oliveira, L. Liebert, A.M. Figueiredo Neto, Liq. Cryst. **5**, 1669 (1989).
7. A.S. Vasilevskaya, E.L. Kitaeva, A.S. Sonin, Russ. J. Phys. Chem. **64**, 599 (1990).
8. Per-Ola Quist, Liq. Cryst. **18**, 623 (1995).
9. C.C. Ho, R.J. Hoetz, M.S. El-Aasser, Langmuir **7**, 630 (1991).
10. A.A. de Melo Filho, A. Lavarde jr., F.Y. Fujiwara, Langmuir **19**, 1127 (2003).
11. C.S. Shih, R. Alben, J. Chem. Phys. **57**, 3055 (1972).
12. R. Alben, Phys. Rev. Lett. **30**, 778 (1973).
13. R. Alben, J. Chem. Phys. **59**, 4299 (1973).
14. Y. Rabin, W.E. McMullen, W.M. Gelbart, Mol. Cryst. Liq. Cryst. **89**, 67 (1982).
15. Z.Y. Chen, J. Deutch, J. Chem. Phys. **80**, 2151 (1984).
16. R. Caflish, Z.-Y. Chen, A. Berker, J. Deutch, Phys. Rev. A **30**, 2562 (1984).
17. A.M. Figueiredo Neto, S.R. Salinas, *The Physics of Lyotropic Liquid Crystals* (Oxford University Press, New York, 2005) pp. 200, 264.
18. P.G. de Gennes, J. Prost, *The Physics of Liquid Crystals* (Clarendon Press, Oxford, 1993) p. 58.
19. G.P. Souza, D.A. Oliveira, D.D. Luders, N.M. Kimura, M. Simões, A.J. Palangana, J. Mol. Liq. **156**, 184 (2010).
20. E. Govers, G. Vertogen, Phys. Rev. A **30**, 1998 (1984).
21. Y. Galerne, J.P. Marcerou, J. Phys. (Paris) **46**, 589 (1985).
22. Y. Galerne, J.P. Marcerou, Phys. Rev. Lett. **51**, 2109 (1983).
23. F.P. Nicoletta, G. Chidichimo, A. Golemme, N. Picci, Liq. Cryst. **10**, 665 (1991).
24. M. Born, E. Wolf, *Principles of Optics*, sixth edition (Pergamon Press, Oxford, 1980) p. 700.
25. M. Laurent, B. Samori, J. Am. Chem. Soc. **109**, 5109 (1987).
26. A. Stroobants, H.N.W. Lekkerkerker, J. Phys. Chem. **88**, 3669 (1984).
27. P. Palffy-Muhoray, J.R. de Bruyn, D.A. Dunmur, J. Chem. Phys. **82**, 5294 (1985).
28. S.R. Sharma, P. Palffy-Muhoray, B. Bergen, D.A. Dunmur, Phys. Rev. A **32**, 3752 (1985).
29. F.M. van der Kooij, H.N.W. Lekkerkerker, Langmuir **16**, 10144 (2000).
30. R.J. Hunter, *Foundations of Colloidal Science*, Vol. **1**, 5th edition (Oxford Science Publications, New York, 1993).
31. E. do Carmo, D.B. Liarte, S.R. Salinas, Phys. Rev. E **81**, 062701 (2010).
32. A.M. Figueiredo Neto, Y. Galerne, A.M. Levelut, L. Liebert, J. Phys. (Paris) Lett. **46**, L-409 (1985).
33. Y. Galerne, A.M. Figueiredo Neto, L. Liebert, J. Chem. Phys. **87**, 1851 (1987).
34. Y. Hendrikx, J. Charvolin, M. Rawiso, Phys. Rev. B **33**, 3534 (1986).